Synthesis of New Indolocarbazole-Acceptor Alternating Conjugated Copolymers and Their Applications to Thin Film Transistors and Photovoltaic Cells

Jung-Hsun Tsai,[†] Chu-Chen Chueh,[†] Mei-Hsiu Lai,[†] Chih-Feng Wang,[†] Wen-Chang Chen,*[,†,‡] Bao-Tsan Ko,[§] and Ching Ting[§]

Department of Chemical Engineering, National Taiwan University, Taipei 106 Taiwan, Institute of Polymer Science and Engineering, National Taiwan University, Taipei 106 Taiwan, and Materials and Chemical Laboratories, Industrial Technology Research Institute, Hsinchu, Taiwan 300

Received December 4, 2008; Revised Manuscript Received January 17, 2009

ABSTRACT: We report synthesis, properties, and optoelectronic device characteristics of six new indolocarbazole−acceptor conjugated copolymers prepared by Suzuki coupling reaction. Two different linkages of indolocarbazole (**28IC** and **39IC**) and four acceptors of 2,3-didodecylthieno[3,4-*b*]pyrazine (**TP12**), 2,3-bis(4-(2-ethylhexyloxy) phenyl)thieno[3,4-*b*]pyrazine (**TPO**), 2,1,3-benzothiadiazole (**BT**), and 2,3-bis(4-(2-ethylhexyloxy)phenyl)quinoxaline (**QO**) were used to explore the effects of acceptor structure, linkage, and side group on the electronic and optoelectronic properties. The optical band gap (eV) of the studied copolymers were in the following order: **P28IC-TPO** (1.58) < **P39IC-TP12** (1.79) < **P28IC-TP12** (1.84) < **P28IC-BT** (2.09) < **P28IC-QO** (2.31) < **P39IC-QO** (2.34). The hole mobility and on−off ratios of the studied copolymers were in the ranges 1.66×10^{-5} to 4×10^{-4} $cm^2/V \cdot s$ and 40−46900, respectively. It basically depended on the degree of intromolecular charge transfer between indolocarbazole and acceptor as well as the HOMO level. The power conversion efficiency (PCE) of the indolocarbazole−acceptor polymer/$PC_{61}BM$ or $PC_{71}BM$ based photovoltaic cells were in the range 0.14−1.40% under the illumination of AM 1.5G (100 mW/cm^2). **P28IC-QO** showed the best PCE among the studied copolymers because of its suitable HOMO/LUMO energy level, high molecular weight, good hole mobility, efficient PL quenching, and large V_{oc}.

Introduction

Donor−acceptor (D−A) conjugated copolymers have attracted extensive research interest because of their tunable electronic and optoelectronic properties through intramolecular charge transfer (ICT).[1,2] Various device applications have been explored for such conjugated copolymers, including light emitting diodes (LEDs),[3−7] photovoltaic cells,[8−24] field-effect transistors (FETs),[25−35] electrochromic devices,[36−38] and memory devices.[39,40]

Among the D−A alternating conjugated polymers, the electron-donating moieties of fluorene,[3−7,18] thiophene,[21−23,28−34] dialkoxylphenylene,[30,41−43] carbazole,[44,45] and cyclopentadithiophene[20,21] have been reported. The TFT and photovoltaic characteristics could be manipulated through the donor/acceptor structure and backbone planarity.[26,25] Indolocarbazole-based materials have emerged as new p-type organic semiconductors due to their relatively low-lying HOMO, thermal stability, and charge carrier mobility.[46−56] The reactive groups at the 2,8- or 3,9-linkages of indolocarbazole also allow the flexibility on exploring new polymer structures. Relatively high hole mobilities of 0.2 and 0.02 $cm^2\ V^{-1}\ s^{-1}$ were reported for the indolo[3,2-*b*]carbazole[49,53,54] and polymer derivatives,[55] respectively. Also, copolymers of indolo[3,2-*b*]carbazole with thiophene or 3,4-ethylenedioxythiophene exhibited the high electrical conductivity.[48] However, the synthesis and properties of indolocarbazole−acceptor conjugated copolymers have not been fully explored yet.

In this study, we report the synthesis, properties and optoelectronic device applications of six indolocarbazole−acceptor conjugated copolymers, including poly[2,8-(5,11-di(2-ethylhexyl)indolo[3,2-*b*]carbazole)-*alt*-5,7-(2,3-didodecylthieno[3,4-*b*]pyrazine)] (**P28IC-TP12**), poly[2,8-(5,11-di(2-ethylhexyl)indolo[3,2-*b*]carbazole)-*alt*-5,7-(2,3-bis(4-(2-ethylhexyloxy)phenyl)-thieno[3,4-*b*]pyrazine)] (**P28IC-TPO**), poly[2,8-(5,11-di(2-ethylhexyl)indolo[3,2-*b*]carbazole)-*alt*-4,7-(2,1,3-benzothiadiazole)] (**P28IC-BT**), poly[2,8-(5,11-di(2-ethylhexyl)indolo[3,2-*b*]carbazole)-*alt*-5,8-(2,3-bis(4-(2-ethylhexyloxy)phenyl)quinoxaline)] (**P28IC-QO**), poly[3,9-(5,11-di(2-ethylhexyl)- indolo[3,2-*b*]carbazole)-*alt*-5,7-(2,3-didodecylthieno[3,4-*b*]pyrazine)] (**P39IC-TP12**), and poly[3,9-(5,11-di(2-ethylhexyl) indolo[3,2-*b*]carbazole)-*alt*-5,8-(2,3-bis(4-(2-ethylhexyloxy)phenyl)quinoxaline)] (**P39IC-QO**). These polymers were synthesized by Suzuki coupling reaction, as shown in Scheme 1. The effects of acceptor type, side group, and linkage (2,8- and 3,9-linkage) on the electronic and optoelectronic properties of the synthesized polymers were explored. The field-effect carrier mobility was obtained from the bottom gate thin film transistor (TFT) devices and correlated with the polymer structures or morphology. Polymer solar cell devices were fabricated by spin-coating polymer blend of indolocarbazole−acceptor copolymer/[6,6]-phenyl-C61-butyric acid methyl ester ($PC_{61}BM$) or 1-(3-methoxycarbonyl)propyl-1-phenyl-[6,6]-C-71 ($PC_{71}BM$), sandwiched between a transparent anode (ITO) and cathodes (Ca/Al). The present study suggested the importance of donor/acceptor structure, linkage position, and HOMO/LUMO energy levels on the characteristics of TFT and photovoltaic cells.

Experimental Section

Materials. 4-Bromophenylhydrazine hydrochloride, 3-Bromophenylhydrazine hydrochloride, cyclohexane-1,4-dione, tetrakis(triphenylphosphine)-palladium(0) [$(PPh_3)_4Pd(0)$], trioctylmethyl ammonium chloride (Aliquat 336), phenyl boronic acid, and bromobenzene

* To whom all correspondence should be addressed. E-mail: chenwc@ntu.edu.tw.
[†] Department of Chemical Engineering, National Taiwan University.
[‡] Institute of Polymer Science and Engineering, National Taiwan University.
[§] Materials and Chemical Laboratories, Industrial Technology Research Institute.

10.1021/ma802720n CCC: $40.75
Published on Web 02/19/2009

Scheme 1. Synthetic Scheme of Indolocarbazole-Based Donor−Acceptor Alternating Conjugated Copolymers

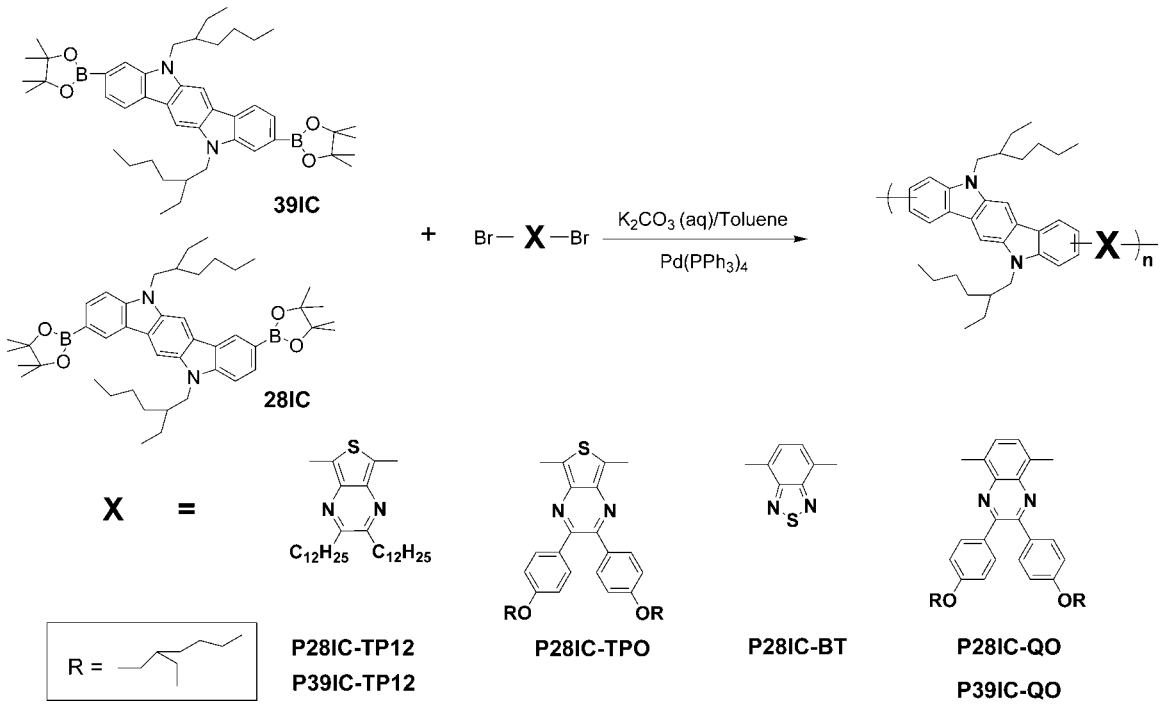

were purchased from Aldrich (Missouri,USA) and used without further purification. Ultra-anhydrous solvents and common organic solvents were purchased from Tedia, Merck, and J.T. Baker. The following donor and acceptor monomers were prepared according to literature procedures: 3,9-bis(4,4,5,5-tetramethyl-1,3,2-dioxaborolan-2-yl)-5,11-di(2-ethylhexyl)indolo[3,2-*b*]carbazole (**39IC**),[48,56] 2,8-bis(4,4,5,5-tetramethyl-1,3,2−dioxaboro-lan-2-yl)-5,11-di(2-ethy-lhexyl)indolo[3,2-*b*]carbazole (**28IC**),[48,56] 5,7-dibromo-2,3-didodecylthieno[3,4-*b*]pyrazine (**TP12**),[29] 2,3-bis(4-(2-ethylhexyloxy)phenyl)-5,7-dibromothieno[3,4-*b*]pyrazine (**TPO**),[57] 4,7-dibromo-2,13-benzothiadiazole (**BT**),[5] and 2,3-bis(4-(2-ethylhexyloxy)phenyl)-5,8-dibromoquinoxaline (**QO**).[58][6,6]-Phenyl-C61-butyric acid methyl ester ($PC_{61}BM$) and 1-(3-methoxycarbonyl)propyl-1-phenyl-[6,6]-C-71 ($PC_{71}BM$) were purchased from Nano-C and Solenne, respectively.

General Procedures of Polymerization. The general procedure of synthesizing indolocarbazole−acceptor alternating copolymers is shown in Scheme 1. Donor monomers (**28IC** or **39IC**), acceptor monomers (**TP12**, **TPO**, **BT**, or **QO**), and tetrakis(triphenylphosphine)palladium(0) (1 mol % with respect to diborate monomer) were dissolved in a mixture of toluene and aqueous 2 M K_2CO_3 (3/2 volume ratio) with several drops of Aliquat 336. The mixture was refluxed under vigorous stirring for 72 h under a nitrogen atmosphere. The end groups were capped by refluxing for 12 h each with phenyl boronic acid and bromobenzene (both 1.1 equiv with respect to diborate monomer). After end-capping, the mixture was cooled and poured into a mixture of methanol and water. The precipitated material was dissolved into a small amount of THF and then reprecipitated into methanol to afford a crude polymer. The crude polymer was washed for 24 h with acetone to remove oligomers and catalyst residues.

Poly[2,8-(5,11-di(2-ethylhexyl)indolo[3,2-*b*]carbazole)-*alt*-5,7-(2,3-didodecylthieno- [3,4-*b*]pyrazine)] (P28IC-TP12). A 512.9 mg (0.70 mmol) sample of **28IC** and 441.4 mg (0.70 mmol) of **TP12** and 10 mL of toluene were used to afford a purple solid (yield: 60%). ^{1}H NMR (CD_2Cl_2), δ (ppm): 9.11 (br, 2H), 8.52 (br, 2H), 8.15 (br, 2H), 7.49 (br, 2H), 4.33 (br, 4H), 3.02 (br, 4H), 2.27 (br, 2H), 2.06 (br, 4H), 1.70−1.06 (m, br, 52H, $-CH_2$), 1.06−0.69 (m, br, 18H, $-CH_3$). Anal. Calcd for $(C_{64}H_{92}N_4S)_n$: C, 80.96; H, 9.77; N, 5.90; S, 3.38. Found: C, 79.75; H, 9.78; N, 5.40; S, 3.08. Weight average molecular weight (M_w) and polydispersity index (PDI) estimated from GPC are 6785 and 1.37, respectively.

Poly[2,8-(5,11-di(2-ethylhexyl)indolo[3,2-*b*]carbazole)-*alt*-5,7-(2,3-bis(4-(2-ethylhexyloxy)phenyl)thieno[3,4-*b*]pyrazine)] (P28IC-TPO). A 527.5 mg (0.72 mmol) sample of **28IC** and 505.9 mg (0.72 mmol) of **TPO** and 10 mL of toluene were used to afford a green solid (yield: 58%). ^{1}H NMR (CD_2Cl_2), δ (ppm): 9.20−6.35 (m, br, 16H, aromatic hydrogens), 4.32 (br, 4H), 3.93 (br, 4H), 2.27 (br, 2H), 2.18−0.25 (br, m, 58H). Anal. Calcd. for $(C_{68}H_{83}N_4SO_2)_n$: C, 80.03; H, 8.20; N, 5.49; S, 3.14. Found: C, 78.95; H, 8.16; N, 5.24; S, 3.00. Weight average molecular weight (M_w) and polydispersity index (PDI) estimated from GPC are 21660 and 2.30, respectively.

Poly[2,8-(5,11-di(2-ethylhexyl)indolo[3,2-*b*]carbazole)-*alt*-4,7-(2,1,3-benzothiadiazole)] (P28IC-BT). A 732.6 mg (1.0 mmol) sample of **28IC** and 294.0 mg (1.0 mmol) of **BT** and 10 mL of toluene were used to afford a ed solid (yield: 75%). ^{1}H NMR ($CDCl_3$), δ (ppm): 8.85 (br, 2H), 8.16 (br, 4H), 8.02 (br, 2H), 7.60 (br, 2H), 4.36 (br, 4H), 2.30 (br, 2H), 1.68−1.13 (m, br, 16H, $-CH_2$), 1.13−0.75 (m, br, 12H, $-CH_3$). Anal. Calcd for $(C_{40}H_{44}N_4S)_n$: C, 78.39; H, 7.24; N, 9.14; S, 5.23. Found: C, 77.06; H, 7.35; N, 8.64; S, 5.06. Weight average molecular weight (M_w) and polydispersity index (PDI) estimated from GPC are 3140 and 1.32, respectively.

Poly[2,8-(5,11-di(2-ethylhexyl)indolo[3,2-*b*]carbazole)-*alt*-5,8-(2,3-bis(4-(2-ethylhexyloxy)phenyl)quinoxaline)] (P28IC-QO). A 1099 mg (1.5 mmol) sample of **28IC** and 1044.8 mg (1.5 mmol) of **QO** and 15 mL of toluene were used to afford an orange solid (yield: 64%). ^{1}H NMR (CD_2Cl_2), δ (ppm): 8.84 (br, 2H), 8.26 (br, 2H), 8.19−8.01 (m, br, 4H), 7.75−7.55 (m, br, 4H), 7.50 (br, 2H), 6.84 (br, 4H), 4.46 (br, 4H), 3.92 (br, 4H), 2.35 (br, 2H), 1.68 (br, 2H), 1.61−1.13 (m, br, 32H, $-CH_2$), 1.13−0.65 (m, br, 24H, $-CH_3$). Anal. Calcd for $(C_{70}H_{86}N_4O_2)_n$: C, 82.80; H, 8.54; N, 5.52. Found: C, 81.06; H, 8.55; N, 5.33. Weight average molecular weight (M_w) and polydispersity index (PDI) estimated from GPC are 10560 and 2.15, respectively.

Poly[3,9-(5,11-di(2-ethylhexyl)indolo[3,2-*b*]carbazole)-*alt*-5,7-(2,3-didodecylthieno[3,4-*b*]pyrazine)] (P39IC-TP12). A 732.7 mg (1 mmol) sample of **39IC** and 630.6 mg (1 mmol) of **TP12** and 12 mL of toluene were used to afford a purple solid (yield: 63%). ^{1}H NMR (CD_2Cl_2), δ (ppm): 8.80−7.09 (m, br, 8H), 4.27 (br, 4H),

3.00 (br, 4H), 2.26 (br, 2H), 2.01 (br, 4H), 1.72−1.06 (m, br, 52H, $-CH_2$), 1.06−0.41 (m, br, 18H, $-CH_3$). Anal. Calcd for $(C_{64}H_{92}N_4S)_n$: C, 80.96; H, 9.77; N, 5.90; S, 3.38. Found: C, 79.39; H, 9.70; N, 5.52; S, 3.03. Weight average molecular weight (M_w) and polydispersity index (PDI) estimated from GPC are 9095 and 1.50, respectively.

Poly[3,9-(5,11-di(2-ethylhexyl)indolo[3,2-*b*]carbazole)-*alt*-5,8-(2,3-bis(4-(2-ethylhexyloxy)phenyl)quinoxaline)] (P39IC-QO). A 693.3 mg (0.95 mmol) sample of **39IC** and 659.1 mg (0.95 mmol) of **QO** and 10 mL of toluene were used to afford an orange solid (yield: 70%). ^{1}H NMR (CD_2Cl_2), δ (ppm): 8.50−7.74 (br, m, 10H), 7.73−7.50 (m, br, 4H), 7.01−6.70 (m, br, 4H), 4.45 (br, 4H), 3.86 (br, 4H), 2.34 (br, 2H), 1.72 (br, 2H), 1.65−1.28 (m, br, 32H, -CH_2), 1.28−0.40 (m, br, 24H, $-CH_3$). Anal. Calcd for $(C_{70}H_{86}N_4O_2)_n$: C, 82.80; H, 8.54; N, 5.52. Found: C, 81.57; H, 8.40; N, 5.13. Weight average molecular weight (M_w) and polydispersity index (PDI) estimated from GPC are 10680 and 1.74, respectively.

Characterization. ^{1}H NMR spectra were recorded by Bruker Avance DRX 500 MHz. Gel permeation chromatographic (GPC) analysis was performed on a Laboratory Alliance RI2000 instrument (two column, MIXED-C and D from Polymer Laboratories) connected with one refractive index detector from Schambeck SFD Gmbh. All GPC analyses were performed on polymer/THF solution at a flow rate of 1 mL/min at 40 °C and calibrated with polystyrene standards.

Thermogravimetric analysis (TGA) and differential scanning calorimetry (DSC) measurements were performed under a nitrogen atmosphere at a heating rate of 20 and 10 °C/min using a TA instrument (TGA-951 and DSC-910S), respectively. Atom force microscopy (AFM) measurements were obtained with a NanoScope IIIa AFM (Digital Instruments, Santa Barbara, CA) at room temperature. Commercial silicon cantilevers (Nanosensors, Germany) with typical spring constants of 21−78 N·m^{-1} was used to operate the AFM in tapping mode. Images were taken continuously with the scan rate of 1.0 Hz.

Absorption and photoluminescence (PL) spectra were recorded with a Jasco model UV/vis/NIR V-570 spectrometer and Fluorolog-3 spectrofluorometer (Jobin Yvon), respectively. For the thin film spectra, polymers were first dissolved in dichlorobenzene (8 mg/ml) and filtered through 0.45 μm pore size PTFE membrane syringe filters, spin-coated at a speed rate of 1000 rpm for 60 s onto quartz substrate. Cyclic voltammetry (CV) was performed with the use of a three-electrode cell in which ITO (polymer films area about 0.5 × 0.7 cm^2) was used as a working electrode. A platinum wire was used as an auxiliary electrode. All cell potentials were taken with the use of a homemade Ag/AgCl, KCl (sat.) reference electrode. The energy levels of HOMO were determined from the onset oxidation (E_{onset}^{ox}) and estimated on the basis of the reference energy level of ferrocene (4.8 V below the vacuum level) according to the following equation: HOMO = $-e(E_{onset}^{ox} - E_{ferrocene}^{1/2} + 4.8)$ (eV). The LUMO levels were estimated from HOMO values and values of optical band gaps according to the equation: LUMO = HOMO + E_g^{opt} (eV).[59]

Fabrication and Characterization of Thin Film Transistors. Organic thin film transistors were prepared from polymer thin films with a bottom-contact configuration on the heavily n-doped silicon wafers. A thermally grown 200 nm SiO_2 used as the gate dielectric with a capacitance of 17 nF/cm^2. The aluminum was used to create a common bottom-gate electrode. The source/drain regions were defined by a 100 nm thick gold contact electrode through a regular shadow mask, and the channel length (L) and width (W) were 25 μm and 500 or 100 μm, respectively. Afterward, the substrate was modified with octyltrichlorosilane (OTS) as silane coupling agents. Polymer solution with a concentration of 0.5 wt % in chlorobenzene was filtered through a 0.20 μm pore size PTFE membrane syringe filter. It was then spin-coated onto the silanized SiO_2/Si substrate at a speed rate of 1000 rpm for 60 s and cured at 60 °C overnight in vacuum. Output and transfer characteristics of the FET devices were measured using Keithley 4200 semiconductor parametric analyzer. All the procedures and electrical measurements were performed in ambient air.

Fabrication and Characterization of Polymer Photovoltaic Cells. All the bulk-heterojunction photovoltaic cells were prepared using the same preparation procedures and device fabrication procedure referring as following: The glass−indium tin oxide (ITO) substrates (obtained from Sanyo, Japan (8Ω/□) were first patterned by lithograph, then cleaned with detergent, and ultrasonicated in acetone and isopropyl alcohol, and subsequently dried on hot plate at 120 °C for 5 min, and finally treated with oxygen plasma for 5 min. Poly(3,4-ethylenedioxythiophene):poly(styrenesulfonate) (PEDOT:PSS, Baytron P VP AI4083) was passed through a 0.45 μm filter before being deposited on ITO with a thickness around 30 nm by spin coating at 3000 rpm in the air and dried at 150 °C for 30 min inside a glovebox. The thin film of the polymer/PCBM blends on the top of PEDOT:PSS layer was prepared by spin coating from dichlorobenzene solution. After that, the device was annealing at 110 °C for 20 min in a glovebox. Subsequently, the device was completed by coating 30 nm thickness of Ca and a 130 nm thickness of Al under <10^{-6} torr pressure respectively. The active area of the device is 4 mm^2.

The current−voltage ($J-V$) measurement of the polymer photovoltaic cells was conducted by a computer-controlled Keithley 2400 source measurement unit (SMU) with a Peccell solar simulator under the illumination of AM 1.5G, 100 mW/cm^2. The illumination intensity was calibrated by a standard Si photodiode detector with KG-5 filter.

Results and Discussion

Polymer Structure. The chemical structures of the synthesized polymers are confirmed by NMR and elemental analysis. Figure 1 shows ^{1}H NMR spectrum of the polymer, **P28IC-TP12**, in CD_2Cl_2. The four peaks at 9.11, 8.52, 8.15, and 7.49 ppm are assigned to the protons on the aromatic rings of indolocarbazole, which are similar to the proton peaks of 2,8-based poly(indolo[3,2-*b*]carbazoles)s.[55] The peaks between 4.40 and 0.69 ppm are attributed to the protons on the dodecyl and 2-ethylhexyl side chains. The number of aromatic and aliphatic protons estimated from integration of peak is in a good agreement with the molecular structures of the copolymers. The ^{1}H NMR spectra of the other studied polymers are also consistent with the proposed polymer structures, as shown in the Figures S1−S5 of the Supporting Information. Furthermore, the experimental carbon contents of the prepared polymers are around 1% difference with the theoretical content. The above structural characterization results indicate the successful synthesis of the indolocarbazole−acceptor conjugated copolymers.

All these polymers except **P28IC-BT** are soluble in common solvents, such as chloroform, THF, and 1,2-dichlorobenzene. The good solubility of the synthesized copolymers provides the solution-processed thin films for electronic and optoelectronic applications. The weight-averaged molecular weight and the polydispersity index (M_w, PDI) of the studied polymers, **P28IC-TP12**, **P28IC-TPO**, **P28IC-BT**, **P28IC-QO**, **P39IC-TP12**, and **P39IC-QO** estimated by GPC are (6785, 1.37), (21660, 2.30), (3140, 1.32), (10560, 2.15), (9095, 1.50), and (10680, 1.74), respectively. The low molecular weight of **P28IC-BT** may be due to its poor solubility in THF, but polymer film could be prepared from spin-coating on its polymer solution in dichlorobenzene.

Thermal Stability. Figure 2 shows the thermogravimetric analysis (TGA) curves of the studied copolymers at the heating rate of 20 °C/min under a nitrogen atmosphere. The thermal decomposition temperatures (T_d, 95 wt % residue) of **P28IC-TP12**, **P28IC-TPO, P28IC-BT, P28IC-QO**, **P39IC-TP12,** and **P39IC-QO** are 413, 459, 464, 453, 408, and 471 °C, respectively, which are higher than the poly(indolo[3,2-*b*]carbazole)s with 390 °C.[51] DSC analysis revealed no obvious glass transition temperature for all copolymers, which is probably attributed to the stiff moiety of indolocarbazole.[55] The above thermal analysis

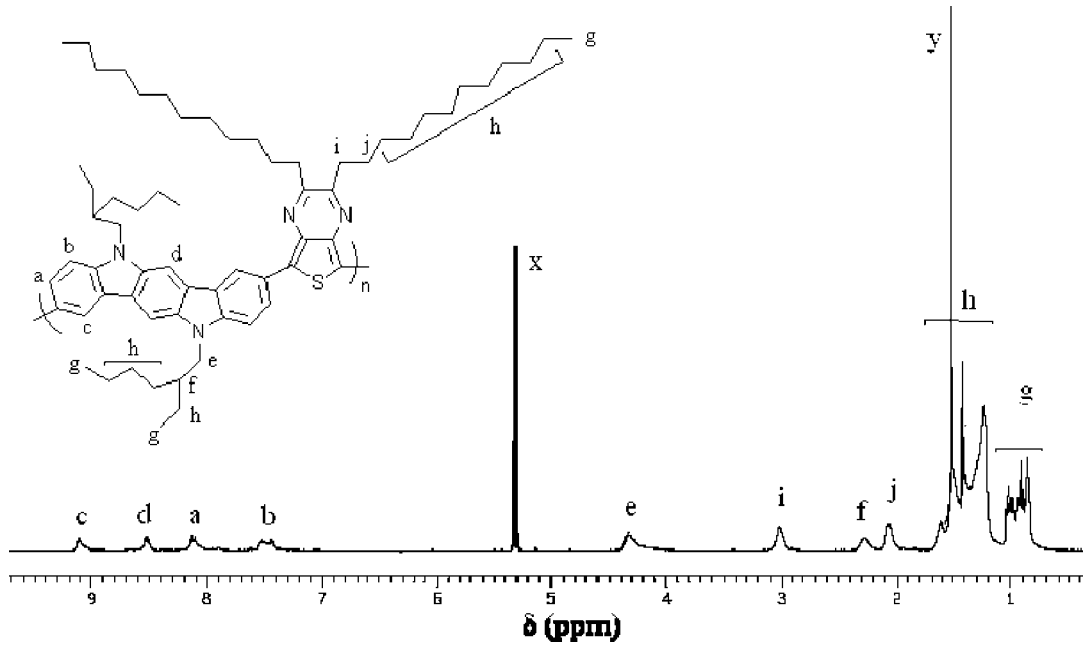

Figure 1. ^{1}H NMR spectrum of **P28IC-TP12** in CD_2Cl_2 solvent (x, CD_2Cl_2; y, H_2O).

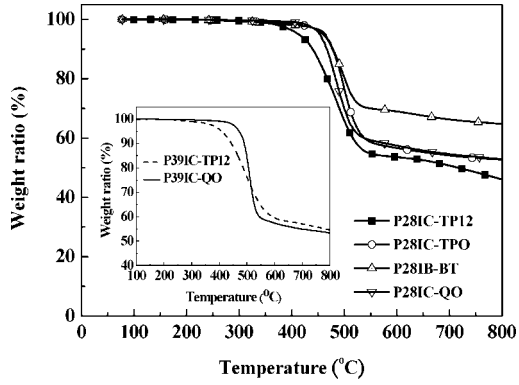

Figure 2. TGA curves of studied copolymers at the heating rate of 20 °C/min under a nitrogen atmosphere.

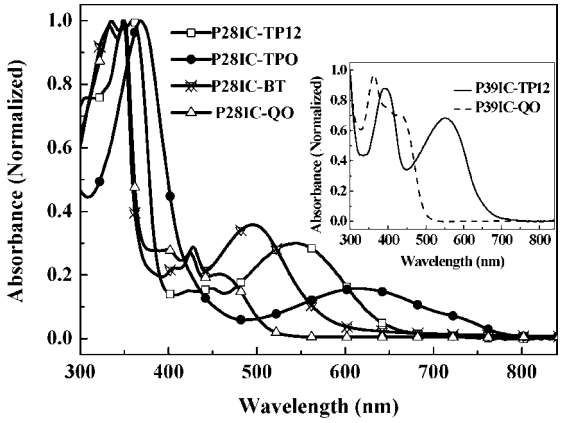

Figure 3. Optical absorption spectra of the studied copolymers in 1,2-dichlorobenzene solutions.

indicates good thermal properties of the studied indolocabazole−acceptor copolymers.

Optical Properties. The UV−vis absorption spectra of the studied copolymers in dilute dichlorobenzene and thin films are shown in Figures 3 and 4, respectively, and the corresponding maximum absorption wavelengths (λ_{max}) are summarized in Table 1. All absorption spectra of these copolymers have two

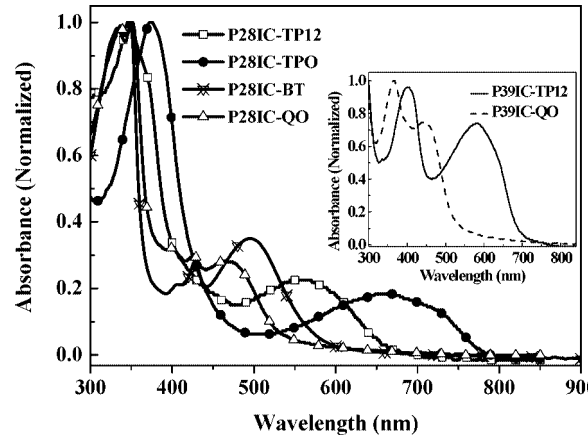

Figure 4. Optical absorption spectra of the studied copolymer films on quartz substrates.

distinct peaks: one in the wavelength range of 420−800 nm and another peak in the wavelength range of 300−420 nm. The λ_{max} in the visible region of **P28IC-TP12**, **P28IC-TPO**, **P28IC-BT**, **P28IC-QO**, **P39IC-TP12**, and **P39IC-QO** in dichlorobenzene solution are observed at 544, 614, 496, 458, 552, and 429 nm, respectively, while those of thin films are shown at 557, 660, 516, 465, 582, and 445 nm. The λ_{max} of the 2,8-linkage poly(indolo[3,2-*b*]carbazole) are around 418−428 nm in THF and 422−435 nm in thin film, respectively, while those of the 3,9-linkage poly(indolo[3,2-*b*]carbazole) are 410−421 nm in THF and 444−477 nm in thin films.[55] By comparing with the λ_{max} of the above indolocarbazole homopolymers in the literature,[47,55] the absorption bands in the wavelength range of 420−800 nm are mostly likely due to the intramolecular charge transfer (ICT) between indolocarbazole and acceptors while those at 300−420 nm are attributed to the indolocarbazole moiety.

The structure-optical property relationships of the studied indolocarbazole−acceptor conjugated copolymers are discussed as below. The optical band gaps (E_g^{opt}, eV) estimated from the absorption edges of thin film spectra are in the following order: **P28IC-TPO** (1.58) < **P39IC-TP12** (1.79) < **P28IC-TP12** (1.89) < **P28IC-BT** (2.09) < **P28IC-QO** (2.31) < **P39IC-QO** (2.34).

Table 1. Optical and Electrochemical Properties of the Studied Indolocarbazole−Acceptor Copolymers

polymer	UV−vis, λ_{max} (nm) in o-DCB	UV−vis, λ_{max} (nm) film	E_g^{opt} (eV)	E_{onset}^{ox} (V)	E_p^{ox} (V)	HOMO[a] (eV)	LUMO[b] (eV)
P28IC-TP12	360, 544	347, 557	1.89	0.56	0.92, 1.17	−4.88	−2.99
P28IC-TPO	368, 614	374, 660	1.58	0.30	1.10, 1.36, 1.90	−4.62	−3.04
P28IC-BT	348, 428, 496	332, 430, 516	2.09	0.58	1.03, 1.83	−4.90	−2.81
P28IC-QO	350, 424, 458	352, 426, 465	2.31	0.79	1.10, 1.70	−5.12	−2.81
P39IC-TP12	391, 552	401, 582	1.79	0.78	1.01, 1.58, 1.79	−5.11	−3.32
P39IC-QO	363, 429	367, 445	2.34	0.76	1.00, 1.67	−5.09	−2.75

[a] HOMO $= -e(E_{onset}^{ox} - E_{ferrocene}^{1/2} + 4.8)$. [b] LUMO $= E_g^{opt}$ − HOMO.

As compared to the previous literature,[5,60] the order of the acceptor strength, **Q** < **TP** < **BT**, is not in agreement with a decreasing trend on the optical band gap of these alternative copolymers. The much lower E_g^{opt} of the **TP**-based copolymers (**P28IC-TP12**, **P28IC-TPO**, and **P39IC-TP12**) than the **BT** or **Q** based copolymers are probably due to the backbone planarity, different conjugation mode of phenyl or thiophene ring, and linkage position. The five-member ring backbone of the thienopyrazine moiety leads to a smaller torsional angle than that of the **BT** or **Q** moiety and promotes the efficient intramolecular charge transfer. Thus, it enhances the double-bond character and leads to an extensive delocalization of the polymer backbone, which leads to the smaller band gap of the **TP**-based copolymers.[5] Furthermore, the much lower E_g^{opt} of **P28IC-TPO** than that of **P28IC-TP12** is due to the incorporation of electron-donating alkoxyphenylene side group on the thienopyrazine moiety of the **P28IC-TPO**, which elevates the HOMO energy level and decreases the band gap. The different linkage effects (2,8- and 3,9-linkage) on the optical properties can be revealed from the comparison of the spectra between **P28IC-TP12** and **P39IC-TP12**. The **P39IC-TP12** has a stronger absorption intensity and more red-shifted peak than the **P28IC-TP12** in the visible region, indicating the higher backbone planarity in the former. Note that the extensive π-conjugation exists along the 3,9-linkage indolocarbazole polymer backbone but the restricted π-conjugation systems is found on the 2,8-linkage copolymers.[55] However, the λ_{max} of **P39IC-QO** shows a slight blue-shift than that of **P28IC-QO,** which exhibits the opposite effect in comparison with those of the **P28IC-TP12**/**P39IC-TP12** and poly(indolo[3,2-*b*]carbazole)s.[47,55] It is probably attributed to the large torsional angle in the polymer backbone resulted from not only the six-member **QO** moiety but also the bulky alkoxyphenylene side chain.[61] Such effect suppressed the linkage position on the degree of π-conjugation in the polymer backbone. However, other factors may contribute to the above opposite trend on the optical properties, such as molecular packing in the polymer film or film quality.

Electrochemical Properties. Parts a and b of Figure 5 show that the cyclic voltammetry (CV) curves of the studied polymers using polymer films in acetonitrile at a potential scan rate of 100 mV/s. The electrochemical characteristics of the onset oxidation (E_{onset}^{ox}), peak oxidation (E_p^{ox}), and the estimated energy levels (HOMO and LUMO) are listed in Table 1. Apparently, these copolymers exhibit reversible oxidative processes expect **P39IC-QO**. The onset oxidation (E_{onset}^{ox}) of the **P28IC-TP12**, **P28IC-TPO**, **P28IC-BT**, **P28IC-QO**, **P39IC-TP12**, and **P39IC-QO** films are observed at 0.56, 0.30, 0.58, 0.79, 0.78, and 0.76 V, respectively. In addition, the corresponding peak oxidation (E_p^{ox}(V)) of **P28IC-TP12**, **P28IC-TPO**, **P28IC-BT**, **P28IC-QO**, **P39IC-TP12**, and **P39IC-QO** are exhibited at (0.92, 1.17), (1.10, 1.36, 1.90), (1.03, 1.83), (1.10, 1.70), (1.01, 1.58, 1.79), and (1.00, 1.67), respectively. The multiple oxidation peaks of the studied copolymers maybe due to the two oxidation positions of the N atom in the indolocarbazole moiety. The HOMO levels estimated from the $E_{onset}^{ox}$of the **P28IC-TP12**, **P28IC-TPO**, **P28IC-BT**, **P28IC-QO**, **P39IC-TP12**, and **P39IC-QO** films are −4.88, −4.62, −4.90, −5.12, −5.11, and −5.09 eV, respectively. The higher HOMO levels of the studied indololocarbazole−acceptor copolymers compared to that of the homopolymers (2,8-linkage poly(indolo[3,2-*b*]carbazole) (−5.24 eV) and 3,9-linkage poly(indolo[3,2-*b*]carbazole) (−5.39 eV)),[51] indicates the strong intramolecular charge transfer effects. For the 2,8-linkage copolymers (**P28IC-TP12**, **P28IC-TPO**, **P28IC-BT**, and **P28IC-QO**), the increase of acceptor strength (**BT** > **TP** > **Q**) not only elevates the HOMO level but also lowers the LUMO level. **P28IC-TPO** (−4.62 eV) has a higher HOMO level than **P28IC-TP12** due to the electron-donating alkoxyphenylene side group. Compared to **P28IC-TP12** (−4.87 eV), **P39IC-TP12** (−5.11 eV) has a lower HOMO level, indicating that 3,9-based copolymers have better air stability than 2,8-based copolymers.[51] However, **P28IC-QO** (−5.12 eV) shows a slightly low-lying HOMO level than **P39IC-QO** (−5.09 eV), which is probably due to the steric hindrance effect discussed in the optical property section.[61]

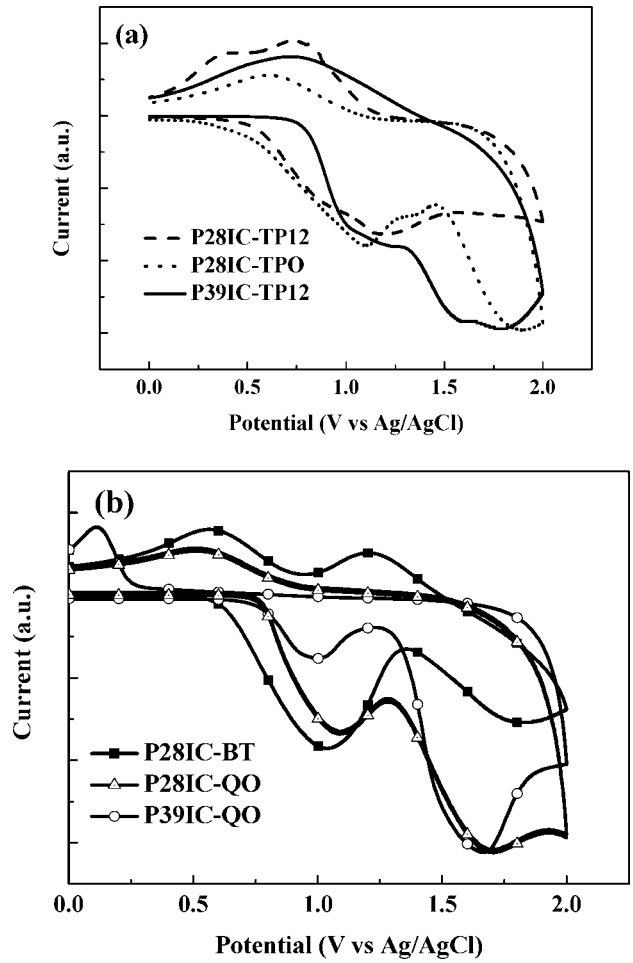

Figure 5. Cyclic voltammograms of studied copolymers thin film in 0.1 M $TBAPF_6$ solution: (a) electrochemical oxidation of **P28IC-TP12**, **P28IC-TPO**, and **P39IC-TP12**; (b) electrochemical oxidation of **P28IC-BT**, **P28IC-QO**, and **P39IC-QO**.

Table 2. Photovoltaic and TFT Characteristics of the Studied Indolocarbazole−Acceptor Copolymers

	TFT−pristine polymer		solar cell−polymer/PCBM (1:4)[c]			
polymer	mobility ($cm^2\ V^{-1}\ s^{-1}$)	on/off	J_{sc} (mA/cm^2)	V_{oc} (V)	FF (%)	PCE[b] (%)
P28IC-TP12	4.04×10^{-4}	236	0.98	0.49	0.45	0.22
P28IC-TPO	5.50×10^{-5}	40	0.98	0.35	0.41	0.14
P28IC-BT	1.93×10^{-4}	30900	2.11	0.55	0.42	0.49
P28IC-QO	1.89×10^{-4}	46900	3.15(4.46)[a]	0.66 (0.65)[a]	0.42 (0.48)[a]	0.87 (1.40)[a]
P39IC-TP12	2.42×10^{-4}	1180	2.45	0.60	0.45	0.66
P39IC-QO	1.66×10^{-5}	50	1.53	0.67	0.32	0.32

[a] Using $PC_{71}BM$ as acceptor. [b] The average value of power conversion efficiency is calculated from 4 pixels in the device. [c] The polymer blend for solar cell device characterization using $PC_{61}BM$ except **P28ICQO** using both $PC_{61}BM$ and $PC_{71}BM$.

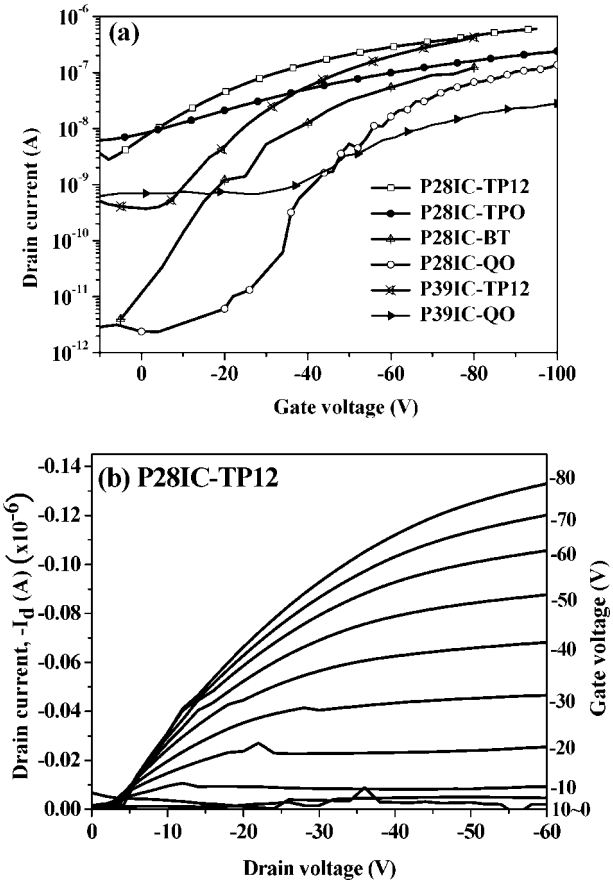

Figure 6. (a) Transfer characteristics of the polymer devices with an OTS-modified surface and annealed at 100 °C, where $V_{ds} = -100$ V. (b) Output characteristic of the **P28IC-TP12** based TFT device.

Polymer Thin Film Transistor Characteristics. The charge transporting characteristics of the studied polymers were explored by their bottom contact thin film transistor (TFT) devices and summarized in Table 2. Figure 6a shows the FET transfer characteristics of the studied copolymer devices on the OTS-modified SiO_2. These polymers show typical p-channel characteristics (drain current (I_d) versus drain voltage (V_d) at various gate voltages (V_g) when operate in the accumulation mode operation. In the saturation region ($V_d > V_g - V_t$), I_d can be described by eq 1:[30]

$$I_d = \frac{WC_o\mu_h}{2L}(V_g - V_t)^2 \quad (1)$$

Here μ_h is the hole mobility, W is the channel width, L is the channel length, and C_o is the capacitance of the gate insulator per unit area (SiO_2, 200 nm, $C_o = 17$ nF/cm^2), respectively. The saturation region mobility of the studied polymers is calculated from the transfer characteristics of TFT involving plotting $(I_d)^{1/2}$ versus V. The hole mobilities of **P28IC-TP12**, **P28IC-TPO**, **P28IC-BT**, and **P28IC-QO** are 4.04×10^{-4}, 5.50×10^{-5}, 1.93×10^{-4}, and 1.89×10^{-4} $cm^2\ V^{-1}\ s^{-1}$, respectively, with their corresponding on/off ratios of 236, 40, 30900, and 46900. The output characteristic of the **P28IC-TP12** polymer device is shown in Figure 6b. The hole mobilities of these 2,8-linkage indolocarbazole−acceptor conjugated copolymers are comparable to the parent 2,8-linkage poly(indolo[3,2-*b*]carbazoles)s synthesized through Zn-mediated dehalogenative coupling polymerization.[55] The order on the charge mobilities ($cm^2\ V^{-1}\ s^{-1}$) is **TP** (4.04×10^{-4}) > **BT** (1.93×10^{-4}) ≅ **Q** (1.89×10^{-4}). It indicates the significance of intermolecular charge transfer on the carrier mobility, which is similar to our previous study on the fluorene based donor−acceptor conjugated copolymers.[28] The poor performance of the **P28IC-TPO** based TFT device is mainly due to the high-lying HOMO level (−4.6 eV), which forms a large hopping barrier with Au (Work function around −5.1 eV) and the possibility of inducing oxygen doping. On the other hand, the hole mobilities of **P39IC-TP12** and **P39IC-QO** are 2.42×10^{-4} and 1.66×10^{-5} $cm^2\ V^{-1}\ s^{-1}$, respectively, with on/off ratios of 1180 and 50. The charge mobilities of the studied 3,9-linkage indolocarbazole−acceptor copolymers significantly enhance in comparison with the parent indolocarbazole homopolymer without hole mobility.[55] The hole mobility of **P28IC-QO** is one-order higher than that of **P39IC-QO** and also has a superior on/off ratio.

Since these two polymers have similar molecular weights and HOMO/LUMO energy levels, it suggests the significance of the linkage effect on carrier mobility. In general, the 2,8-linkage copolymers shows superior TFT performances than 3,9-linkage ones since the former provides a more sufficient resonance to form stable ammonium radical cations.[55] A similar trend is also observed on the comparison of carrier mobility between **P28IC-TP12** and **P39IC-TP12**.

Polymer Photovoltaic Cell Characteristics. The bulk heterojunction solar cell were fabricated with a sandwich structure of ITO/PEDOT:PSS/Polymer:PCBM (1:4, w/w)/Ca (30nm)/Al (130 nm). The *J-V* characteristics of polymer solar cell prepared from the blends of polymer:PCBM (1:4, w/w) are shown in Figure 7. The photovoltaic properties including open-circuit voltage (V_{oc}), short-circuit current (J_{sc}), fill factor (FF), and power conversion efficiency (PCE) are summarized in Table 2. The PCEs (%) of the corresponding polymer/$PC_{61}BM$-based devices are 0.22 (**P28IC-TP12**), 0.14 (**P28IC-TPO**), 0.49 (**P28IC-BT**), 0.87 (**P28IC-QO**), 0.66 (**P39IC-TP12**), and 0.32 (**P39IC-QO**), respectively.

The PCE of the above photovoltaic cells are discussed based on the following factors. The HOMO and LUMO levels of the studied indolocarbazole−acceptor copolymers and $PC_{61}BM$ are shown in Figure 8. Note that the HOMO/LUMO energy levels are of crucial importance for device performance especially to V_{oc} and charge separation efficiency. For ideal energy levels of polymer used to solar cell application based on PCBM blend system, the LUMO level was suggested to be between −3.7 and −4.0 eV to ensure efficient electron transfer from polymer (donor) to PCBM (acceptor); and the HOMO level was between

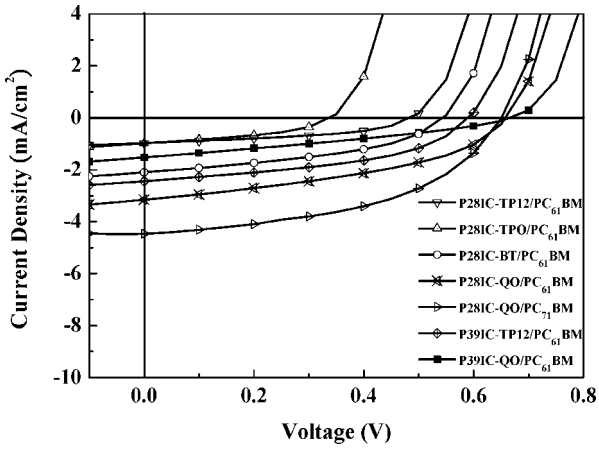

Figure 7. *J*−*V* characteristics of polymer solar cells with polymer:PCBM (1:4, w/w) under the illumination of AM 1.5G, 100 mW/cm^2.

−5.2 and −5.8 eV to take solar emission spectrum and open circuit voltage into account.[45] As shown in Table 2, the V_{oc} of the photovoltaic devices increases from 0.35 (**P28IC-TPO**) to 0.50 (**P28IC-TP12**), 0.55 (**P28IC-BT**), and 0.66 V (**P28IC-QO**). In general, a higher V_{oc} could be resulted from the lower HOMO energy levels of studied copolymers because V_{oc} is related to the energy differences between the HOMO of the donor (conjugated polymer) and the LUMO of the acceptor ($PC_{61}BM$). Such difference on the V_{oc} leads to the variation on the PCE of the studied polymer photovoltaic cells. The lower PCE of the studied polymer photovoltaic cells than those of the poly(2,7-carbazole−acceptor)[45] is probably due to the mismatched HOMO/LUMO energy levels of the former besides the order structure factor.

The steady state of photoluminescence spectra also can be informative for the nature of photoinduced charge transfer on the studied polymer blends. The photoluminescence (PL) spectra of studied polymers and polymer/$PC_{61}BM$ (1:4) in thin films excited at corresponding absorption maxima of studied polymers are presented in Figure 9 (**P28IC-QO**) and those of other polymers are shown in Figure S6 of the Supporting Information. **P28IC-QO** (quenching 99.9%) shows the highest PL quenching ratio than **P28IC-TP12** (quenching 98.1%), **P28IC-TPO** (quenching 91.1%), and **P39IC-QO** (quenching 95.9%). It indicates that photoinduced charge transfer from the **P28IC-QO** to PCBM is much more efficient than those of the **TP**-based copolymers (**P28IC-TP12**/$PC_{61}BM$, **P28IC-TPO**/$PC_{61}BM$, and **P39IC-TP12**/$PC_{61}BM$).

Among 2,8-based copolymers (**P28IC-TP12**, **P28IC-TPO**, **P28IC-BT**, and **P28IC-QO**), **P28IC-QO** shows the best PCE because of its higher molecular weight for film formation, appropriate hole mobility, most efficiently PL quenching, and largest V_{oc} than others. Although **P28IC-TPO** with the lowest band gap enables to collect more photon flux, the lowest PCE is probably due to the lowest hole mobility (5.50×10^{-5} cm^2 V^{-1} s^{-1}) and V_{oc} (0.35 V) among the studied **TP**-based copolymers. The photovoltaic cell fabricated from **BT** based copolymers generally obtained a high PCE, because of its higher structural organization and appropriate energy levels.[20,45] However, the poor solubility of **P28IC-BT** leads to a relatively higher roughness (0.634 nm) among corresponding polymers and restricts its photovoltaic cell performance.

As both copolymers possess similar molecular weights and hole mobilities, the higher PCE of **P39IC-TP12**/$PC_{61}BM$ (0.66%) than that of **P28IC-TP12**/$PC_{61}BM$ (0.22%) may be explained as below: the higher V_{oc} attributed to the lower HOMO level and higher J_{sc} owing to the considerable absorption differences and lowest LUMO level (−3.32 eV) suitable for charge separation. On the contrary, the PCE of **P39IC-QO**/$PC_{61}BM$ (0.32%) is much lower than that of **P28IC-QO**/$PC_{61}BM$ (0.87%), which is due primarily to a remarkable decrease in J_{sc} and FF since molecular weights and V_{oc} of both

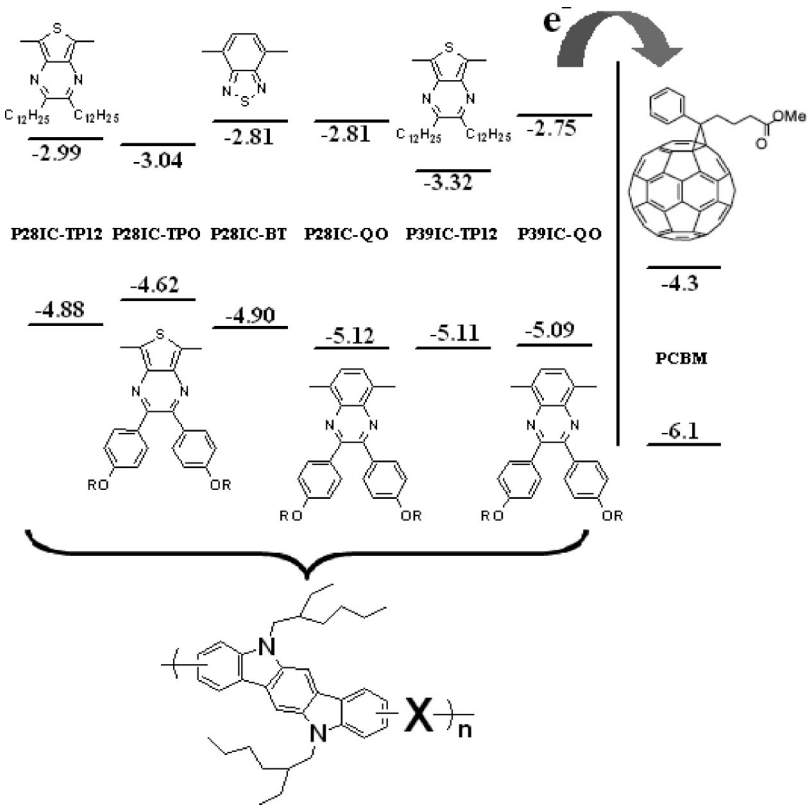

Figure 8. Energy levels for the six indolocarbazole−acceptor copolymers along with the acceptor $PC_{61}BM$.

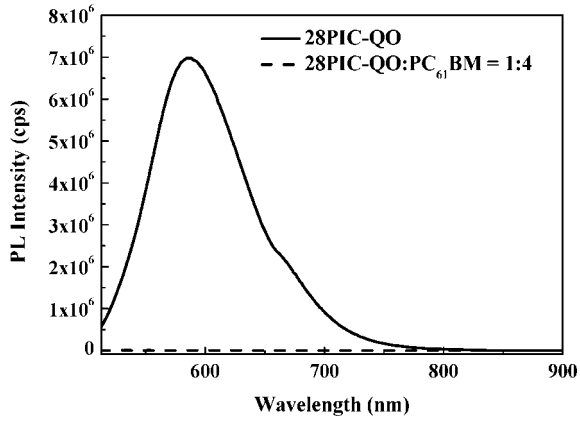

Figure 9. PL spectra of **P28IC-QO** film and a blending film of **P28IC-QO**/$PC_{61}BM$ (1:4 w/w).

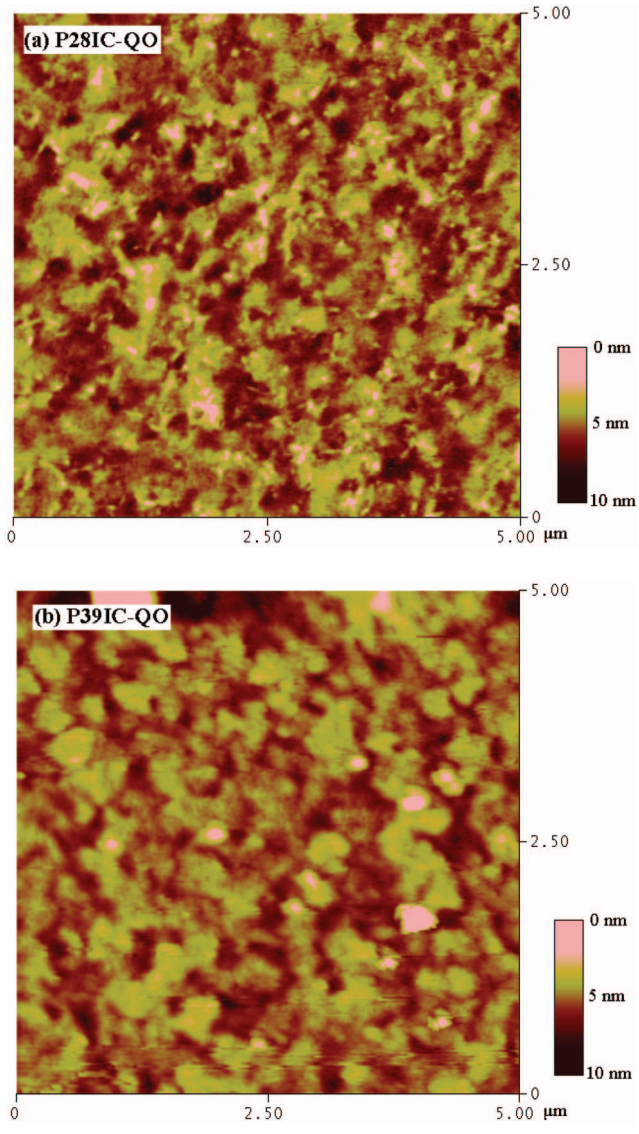

Figure 10. Tapping mode AFM topographies images at 0−10 nm height scale for polymer/$PC_{61}BM$ (1:4) blend films of **P28IC-QO** and **P39IC-QO**.

polymers are comparable. Parts a and b of Figure 10 show AFM images of **P28IC-QO**/$PC_{61}BM$ and **P39IC-QO**/$PC_{61}BM$ blend films. The root mean squares surface roughness (rms) of the two polymer films are comparable (1.04 and 1.09 nm). However, **P28IC-QO**/$PC_{61}BM$ shows a smaller domain size and more well-penetrated morphology than **P39IC-QO**/$PC_{61}BM$ and thus large interfacial areas of **P28IC-QO**/$PC_{61}BM$ leads to improved J_{sc} and FF. Even though **P39IC-QO** has a much higher absorption intensity in the visible region, its relatively lower hole mobility (1.66×10^{-5} cm^2 V^{-1} s^{-1}), less PL quenching efficiency, and higher surface roughness leads to inferior photovoltaic cell performance than **P28IC-QO**. AFM images of other copolymers (Figure S7, see Supporting Information) show relatively small roughness in the range 0.352−0.634 nm of polymer/$PC_{61}BM$ (1:4) thin films, and no significant aggregation is formed. Further enhancement on the PCE of the **P28IC-QO** based photovoltaic cell to 1.40% was achieved if $PC_{71}BM$ was used to replace $PC_{61}BM$ in the blend, as depicted in Table 2. The significantly higher short-circuit current density observed is likely attributed to the considerably higher absorption of $PC_{71}BM$ in the visible region.[11]

The above characteristics of the indolocarbzole−acceptor copolymer based photovoltaic cells reveal the importance of HOMO/LUMO energy levels, carrier mobility, and surface structures on the power conversion efficiency. Thus, the optimization of donor/acceptor structure and linkage lead to the difference on the power conversion efficiency. The incorporation with the **Q** acceptors into the indolocarbazole derivatives makes the best photovoltaic cell performance among the studied copolymers because of good film-forming ability, suitable HOMO level, and most efficiently PL quenching than other acceptors (**TP** and **BT**).

Conclusion

Six indolocarbazole−acceptor copolymers were successfully synthesized by palladium(0)-catalyzed Suzuki coupling reaction and confirmed by NMR and elemental analysis. The copolymers showed a wide range of optical band gaps between 1.58 and 2.31 eV, through the variation of acceptors, linkage, and side groups. The hole mobility of the studied copolymers could be as high as 4×10^{-4} cm^2 V^{-1} s^{-1} with the large on/off ratio $>10^4$. It basically depends on the degree of intromolecular charge transfer and also the HOMO level. The power conversion efficiency (PCE) of the indolocarbazole−acceptor polymer/$PC_{61}BM$ or $PC_{71}BM$ based photovoltaic cells were in the range of 0.14−1.40% under the illumination of AM 1.5G (100 mW/cm^2). The incorporation with the **Q** acceptors into the indolocarbazole derivatives makes the best photovoltaic cell performance among the studied copolymers because of suitable HOMO/LUMO energy level, high molecular weight, good hole mobility, efficient PL quenching, and large V_{oc}.

Acknowledgment. The financial support of the National Science Council (NSC96-2221-E-002-024-MY3), the Excellent Research Projects of National Taiwan University, and the Ministry of Economic Affairs of Taiwan (96-Ec-17-A-08-S1-015) are highly appreciated.

Supporting Information Available: Figures showing ^1H NMR spectra of polymers **P28IC-TPO**, **P28IC-BT**, **P28IC-QO**, **P39IC-TP12** and **P39IC-QO**, PL spectra of polymer film and polymer/PCBM (1:4 w/w) of **P28IC-TP12**, **P28IC-TPO**, **P39IC-TP12**, and **P39IC-QO**, and tapping mode AFM topographies images for polymer/$PC_{61}BM$ (1:4) blend films of **P28IC-TP12**, **P28IC-TPO**, **P28IC-BT**, and **P39IC-TP12**. This material is available free of charge via the Internet at http://pubs.acs.org.

References and Notes

(1) van Mullekom, H. A. M.; Vekemans, J. A. J. M.; Havinga, E. E.; Meijer, E. W. *Mater. Sci. Eng. Rev.* **2001**, *32*, 1.
(2) Tsai, F. C.; Chang, C. C.; Liu, C. L.; Chen, W. C.; Jenekhe, S. A. *Macromolecules* **2005**, *38*, 1958.

(3) Ego, C.; Marsitzky, D.; Becker, S; Zhang, J.; Grimsdale, A. C.; Mullen, K.; MacKenzie, J. D.; Silva, C.; Friend, R. H. *J. Am. Chem. Soc.* **2003**, *125*, 437.
(4) Liu, J; Guo, X.; Bu, L. J.; Xie, Z. Y.; Cheng, Y. X.; Geng, Y. H.; Wang, L. X.; Jing, X. B.; Wang, F. S. *Adv. Funct. Mater.* **2007**, *17*, 1917.
(5) Wu, W. C.; Liu, C. L.; Chen, W. C. *Polymer* **2006**, *47*, 627.
(6) Peng, Q.; Peng, J. B.; Kang, E. T.; Neoh, K. G.; Cao, Y. *Macromolecules* **2005**, *38*, 7292.
(7) Yang, R. Q.; Tian, R. Y.; Yan, J. G.; Zhang, Y.; Tang, J.; Hou, Q.; Yang, W.; Zhang, C.; Cao, Y. *Macromolecules* **2005**, *38*, 244.
(8) Dennler, G.; Scharber, M. C.; Ameri, T.; Denk, P.; Forberich, K.; Waldauf, C.; Brabec, C. J. *Adv. Mater.* **2008**, *20*, 579.
(9) Scharber, M. C.; Muhlbacher, D.; Koppe, M.; Denk, P.; Walfauf, C.; Heeger, A. J; Brabec, C. J. *Adv. Mater.* **2007**, *18*, 794.
(10) Coakley, K. M.; McGehee, M. D. *Chem. Mater.* **2004**, *16*, 4533.
(11) Chen, C. P.; Chan, S. H.; Chao, T. C.; Ting, C.; Ko, B. T. *J. Am. Chem. Soc.* **2008**, *130*, 12828.
(12) Chan, S. H.; Chen, C. P.; Chao, T. C.; Ting, C.; Lin, C. S.; Ko, B. T. *Macromolecules* **2008**, *41*, 5519.
(13) Li, G.; Shrotriya, V.; Huang, J.; Yao, Y.; Moriarty, T.; Emery, K.; Yang, Y. *Nat. Mater.* **2005**, *4*, 864.
(14) Kim, Y.; Cook, S.; Tuladhar, S. M.; Choulis, S. A.; Nelson, J.; Durrant, J. R.; Bradley, D. D. C.; Giles, M.; Mcculloch, I.; Ha, C. S.; Ree, M. *Nat. Mater.* **2006**, *5*, 197.
(15) Peet, J.; Kim, J. Y.; Coates, N. E.; Ma, W. L.; Moses, D.; Heeger, A. J; Bazan, G. C. *Nat. Mater.* **2007**, *6*, 497.
(16) Wong, W. Y.; Wang, X. Z.; He, Z.; Djurisic, A. B.; Yip, C. T.; Cheung, K. Y.; Wang, H.; Mak, C. S. K.; Chan, W. K. *Nat. Mater.* **2007**, *6*, 521.
(17) Campos, L. M.; Tontcheva, A.; Gunes, S.; Sonmez, G.; Neugebauer, H.; Sariciftci, N. S.; Wudl, F. *Chem. Mater.* **2005**, *17*, 4031.
(18) Gadisa, A.; Mammo, W.; Andersson, L. M.; Admassive, S.; Zhang, F.; Andersson, M. R.; Inganäs, O. *Adv. Funct. Mater.* **2007**, *17*, 3836.
(19) Li, Y.; Zou, Y. *Adv. Mater.* **2008**, *20*, 2952.
(20) Soci, C.; Hwang, I. W.; Moses, D.; Zhu, Z.; Waller, D.; Gaudiana, R.; Brabec, C. J.; Heeger, A. J. *Adv. Funct. Mater.* **2007**, *17*, 632.
(21) Moulé, A. J.; Tsami, A.; Bünnagel, T. W.; Forster, M.; Kronenberg, N. M.; Scharber, M.; Koppe, M.; Morana, M.; Brabec, C. J.; Meerholz, K.; Scherf, U. *Chem. Mater.* **2008**, *20*, 4045.
(22) Chang, Y. T.; H; su, S. L.; Su, M. H.; Singh, T. A.; Diau, E. W.-G.; Wei, K. H. *Adv. Funct. Mater.* **2008**, *18*, 2356.
(23) Baek, N. S.; Hau, S. K.; Yip, H. L.; Acton, O.; Chen, K. S.; Jen, A. K. Y. *Chem. Mater.* **2008**, *20*, 5734.
(24) Okamota, T.; Jiang, Y.; Qu, F.; Mayer, A. C.; Parmer, J. E.; McGehee, M. D.; Bao, Z. *Macromolecules* **2008**, *41*, 6977.
(25) Chua, L. L.; Zaumseil, J.; Chang, J. F.; Ou, E. C.; Ho, P. K. H.; Sirringhaus, H.; Friend, R. H. *Nature* **2005**, *434*, 194.
(26) Gadisa, A.; Perzon, E.; Andersson, M. R.; Inganäs, O. *Appl. Phys. Lett.* **2007**, *90*, 113510.
(27) Chen, M. X.; Crispin, X.; Perzon, E.; Andersson, M. R.; Pullerits, T.; Andersson, M.; Inganäs, O.; Berggren, M. *Appl. Phys. Lett.* **2005**, *87*, 252105.
(28) Lee, W. Y.; Cheng, K. F.; Wang, T. F.; Chueh, C. C.; Chen, W. C.; Tuan, C. S.; Lin, J. L. *Macromol. Chem. Phys.* **2007**, *208*, 1909.
(29) Cheng, K. F.; Liu, C. L.; Chen, W. C. *J. Polym. Sci., Part A: Polym. Chem.* **2007**, *45*, 5872.
(30) Liu, C. L.; Tsai, J. H.; Lee, W. Y.; Chen, W. C.; Jenekhe, S. A. *Macromolecules* **2008**, *41*, 6952.
(31) Yamamoto, T.; Kukubo, H.; Kobashi, M.; Sakai, Y. *Chem. Mater.* **2004**, *16*, 4616.
(32) Champion, R. D.; Cheng, K. F.; Pai, C. L.; Chen, W. C.; Jenekhe, S. A. *Macromol. Rapid Commun.* **2005**, *26*, 1835.
(33) Babel, A.; Zhu, Y.; Cheng, K. F.; Chen, W. C.; Jenekhe, S. A. *Adv. Funct. Mater.* **2007**, *17*, 2542.
(34) Zhu, Y.; Champion, R. D.; Jenekhe, S. A. *Macromolecules* **2006**, *39*, 8712.
(35) Zhou, E. J.; Tan, Z.; Yang, Y.; Hou, L. J.; Zou, Y. P.; Yang, C. H.; Li, Y. F. *Macromolecules* **2007**, *40*, 1831.
(36) Sonmez, G. ; Shen, C. K. F.; Rubin, Y.; Wudl, F. *Angew. Chem., Int. Ed.* **2004**, *43*, 1498.
(37) Sonmez, G. ; Sonmez, H. B.; Shen, C. K. F.; Jost, R. W.; Rubin, Y.; Wudl, F. *Macromolecules* **2005**, *38*, 669.
(38) Durmus, A.; Gunbas, G. E.; Toppare, L. *Chem. Mater.* **2007**, *19*, 6247.
(39) Lin, Q. D.; Chang, F. C.; Song, Y.; Zhu, C. X.; Liaw, D. J.; Chan, D. S. H.; Kang, E. T.; Neoh, K. G. *J. Am. Chem. Soc.* **2006**, *128*, 8732.
(40) Chu, C. W.; Ouyang, J.; Tseng, J. H.; Yang, Y. *Adv. Mater.* **2005**, *17*, 1440.
(41) Thompson, B. C.; Kim, Y. G.; mcCarley, T. D.; Reynolds, J. R. *J. Am. Chem. Soc.* **2006**, *128*, 12714.
(42) Yasuda, T.; Imase, T.; Yamamoto, T. *Macromolecules* **2005**, *38*, 7378.
(43) Monkman, A. P.; Palsson, L.; Higgins, R. W. T.; Wang, C.; Bryce, M. R.; Batsanov, A. S.; Howard, J. A. K. *J. Am. Chem. Soc.* **2001**, *124*, 6049.
(44) Blouin, N.; Michaud, A.; Leclerc, M. *Adv. Mater.* **2007**, *19*, 2295.
(45) Blouin, N.; Michaud, A.; Gendron, D.; Wakim, S.; Blair, E.; Neagu-Plesu, R.; Belletete, M.; Durocher, G.; Tao, Y.; Leclerc, M. *J. Am. Chem. Soc.* **2008**, *130*, 732.
(46) Wakim, S.; Bouchard, J.; Simard, M.; Drolet, N.; Tao, Y.; Leclerc, M. *Chem. Mater.* **2004**, *16*, 4386.
(47) Blouin, N.; Michaud, A.; Wakim, S.; Boudreault, P.-L. T.; Leclerc, M.; Vercelli, B.; Zecchin, S.; Zotti, G. *Macromol. Chem. Phys.* **2006**, *207*, 166.
(48) Blouin, N.; Leclerc, M.; Vercelli, B.; Zecchin, S.; Zotti, G. *Macromol. Chem. Phys.* **2006**, *207*, 175.
(49) Boudreault, P.-L. T.; Wakim, S.; Blouin, N.; Simard, M.; Tessier, C.; Tao, Y.; Leclerc, M. *J. Am. Chem. Soc.* **2007**, *129*, 9125.
(50) Boudreault, P.-L. T.; Blouin, N.; Leclerc, M. *Adv. Polym. Sci.* **2008**, *212*, 99.
(51) Wakim, S.; AIch, B. R.; Tao, Y.; Leclerc, M. *Polym. Rev.* **2008**, *48*, 432.
(52) Lu, J.; Liang, F.; Drolet, N.; Ding, J.; Tao, Y.; Movileanu, R. *Chem. Commun.* **2008**, 5315.
(53) Wu, Y.; Li, Y.; Gardner, S.; Ong, B. S. *J. Am. Chem. Soc.* **2005**, *127*, 614.
(54) Li, Y.; Wu, Y.; Gardner, S.; Ong, B. S. *Adv. Mater.* **2005**, *17*, 849.
(55) Li, Y.; Wu, Y.; Ong, B. S. *Macromolecules* **2006**, *39*, 6521.
(56) Yudina, L. N.; Bergman, J. *Tetrahedron* **2003**, *59*, 1265.
(57) Shahid, M.; Ashraf, R. S.; Klemm, E.; Sensfuss, S. *Macromolecules* **2006**, *39*, 7844.
(58) Aldakov, D.; Palacios, M. A.; Anzenbacher, P., Jr. *Chem. Mater.* **2005**, *17*, 5238.
(59) Sun, Q. J.; Wang, H. Q.; Yang, C. H.; Li, Y. F. *J. Mater. Chem.* **2003**, *13*, 800.
(60) Kitamura, C.; Tanaka, S.; Yamashita, Y. *Chem. Mater.* **1996**, *8*, 570.
(61) Roncali, J. *Chem. Rev.* **1997**, *97*, 173.

MA802720N